Published in final edited form as:

Kidney Int. 2020 July ; 98(1): 133–146. doi:10.1016/j.kint.2020.01.033.

A deletion in the N-terminal polymerizing domain of laminin β2 is a new mouse model of chronic nephrotic syndrome.

Steven D. Funk[1], **Raymond H. Bayer**[1], **Karen K. McKee**[2], **Kazushi Okada**[3], **Hiroshi Nishimune**[3], **Peter D. Yurchenco**[2], **Jeffrey H. Miner**[1]

[1]Department of Internal Medicine, Division of Nephrology, Washington University, St. Louis MO, 63110

[2]Department of Pathology and Laboratory Medicine, Robert Wood Johnson Medical School, Rutgers University, Piscataway, NJ

[3]Department of Anatomy and Cell Biology, University of Kansas School of Medicine, Kansas City, KS

Abstract

The importance of the glomerular basement membrane (GBM) in glomerular filtration is underscored by the manifestations of Alport and Pierson syndromes, caused by defects in type IV collagen α3α4α5 and the laminin β2 chain, respectively. *Lamb2* null mice, which model the most severe form of Pierson syndrome, exhibit proteinuria prior to podocyte foot process effacement and are therefore useful for studying GBM permselectivity. We hypothesize that some *LAMB2* missense mutations that cause mild forms of Pierson syndrome induce GBM destabilization with delayed effects on podocytes. While generating a CRISPR/Cas9-mediated analogue of a human *LAMB2* missense mutation in mice, we identified a 44-amino acid deletion (LAMB2-Del44) within the laminin N-terminal domain, a domain mediating laminin polymerization. Laminin heterotrimers containing LAMB2-Del44 exhibited a 90% reduction in polymerization *in vitro* that was partially rescued by type IV collagen and nidogen. Del44 mice showed albuminuria at 1.8-6.0 g/g creatinine (ACR) at one to two months, plateauing at an average 200 g/g ACR at 3.7 months, when GBM thickening and hallmarks of nephrotic syndrome were first observed. Despite the massive albuminuria, some Del44 mice survived for up to 15 months. Blood urea nitrogen was modestly elevated at seven-nine months. Eight to nine-month-old Del44 mice exhibited glomerulosclerosis and interstitial fibrosis. Similar to *Lamb2*$^{-/-}$ mice, proteinuria preceded foot process effacement. Foot processes were widened but not effaced at one-two months despite the high ACRs. At three months some individual foot processes were still observed amid widespread

Correspondence: Dr. Jeffrey H. Miner, Division of Nephrology, Washington University School of Medicine, 4523 Clayton Ave., Campus Box 8126, St. Louis, MO 63110. minerj@wustl.edu.

DISCLOSURE

None.

Supplementary information is linked to the online version of the paper at www.kidney-international.org.

effacement. Thus, our chronic model of nephrotic syndrome may prove useful to study filtration mechanisms, long-term proteinuria with preserved kidney function, and to test therapeutics.

Graphical Abstract

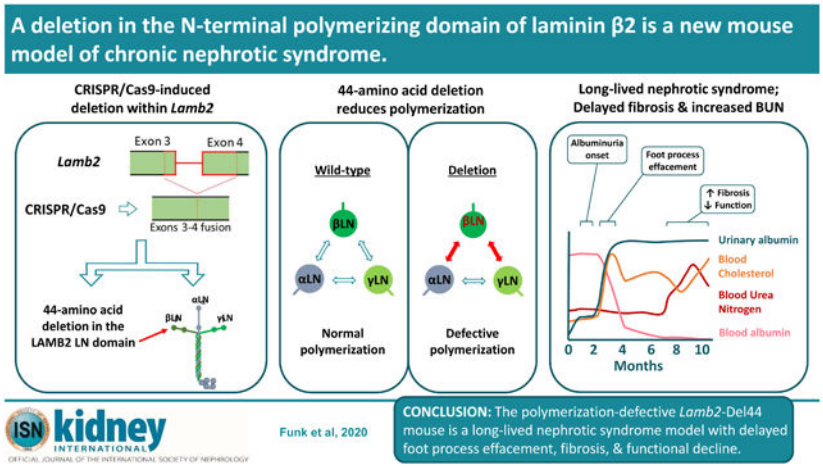

Keywords

Glomerular basement membrane; nephrotic syndrome; Pierson syndrome; laminin

INTRODUCTION

The renal glomerulus is a tuft of capillaries inside Bowman's capsule, which is contiguous with the nephron's downstream tubular segments that modify the glomerular ultrafiltrate to make urine. Glomerular capillaries are comprised of fenestrated endothelium, the glomerular basement membrane (GBM), and a layer of specialized mural epithelial cells called podocytes. Collectively, these three components form a filtration barrier that permits passage of small molecules less than ~60 kD and restricts the passage of large proteins and cells[1]. Podocytes and glomerular endothelial cells secrete and attach to GBM components, predominately via integrin-based adhesive complexes.[2,3] Podocytes produce primary cellular extensions that branch into secondary extensions, termed foot processes, which interdigitate with those of neighboring podocytes and form a unique cell-cell junction called the slit diaphragm.[4] Blood plasma filtered through the filtration barrier into Bowman's space is the "ultrafiltrate".

Glomerular filtration is abnormal when the filtration apparatus is compromised by defects in podocytes, endothelial cells, or the GBM, resulting in leakage of larger proteins (such as albumin and immunoglobulins) into Bowman's space and increased protein quantities in the urine (proteinuria). Progressive proteinuria is typically accompanied by slit diaphragm loss and podocyte foot process effacement. In contrast, other than stereotypical GBM abnormalities found in Alport syndrome and diabetic kidney disease, alterations in GBM architecture are not usually observed when glomerular permselectivity is impaired. Glomerular diseases that are unresolved by treatment with steroids and/or

immunosuppression typically progress to nephrotic syndrome prior to renal failure.[5,6] The hallmark features of nephrotic syndrome are proteinuria >2 g/day, hypoalbuminemia, hyperlipidemia, and edema.[6] The complications of nephrotic syndrome promote life-threatening thrombosis, sudden cardiac death, and arterial disease, among other complications.[5,6] Although angiotensin converting enzyme inhibitors may slow progression, [7] no therapy exists to directly halt or reverse glomerular dysfunction.

Steroid resistant/refractory nephrotic syndrome can be secondary to systemic conditions (e.g., diabetes, lupus, infection, toxins) or caused by mutations.[5,6] Many of these mutations cause loss of podocyte proteins that are either associated with the slit diaphragm or with the cytoskeleton.[8] Pathogenic mutations leading to loss of podocyte-derived extracellular matrix proteins affect GBM constituents, in particular the collagen IV α3, α4, and α5 chains (in Alport syndrome) and the laminin β2 chain (in Pierson syndrome).[9] The exact mechanism by which GBM composition, podocytes, and endothelial cells determine glomerular permselectivity represents a gap in our understanding of glomerular function that is reflected in part by the lack of nephrotic syndrome therapeutics.

Basement membranes are multi-molecular structures with diverse functions that underlie epithelium and endothelium and surround muscle cells, adipose cells, and nerves.[10] Basement membranes are built from four major protein types: laminins, type IV collagens, nidogen, and heparan sulfate proteoglycans.[10] Laminins form heterotrimeric molecules from α, β, and γ chains (e.g., LM-α5β2γ1 (LM-521) in the GBM) inside cells that polymerize into extracellular networks after secretion. Heterotrimers are linked via a coiled-coil in the carboxy end “long arms”, allowing unrestricted movement of amino end “short arms”, each of which contains a laminin NH2-terminal (LN) domain that facilitates laminin polymerization.[11,12]

The developing GBM is initially constructed with LM-511 and LM-111, but isoform transitions during glomerulogenesis lead to primarily LM-521 at maturity.[13-15] Null-mutations in human *LAMB2* (and murine *Lamb2*) eliminate production of LM-521.[16-18] The murine null phenotype is consistent with Pierson syndrome, including congenital nephrotic-range proteinuria, diffuse mesangial sclerosis, ocular abnormalities, muscle weakness, and early death.[16,19] *Lamb2*−/− mice exhibit a unique delay in podocyte foot process effacement relative to the progression of proteinuria,[20] indicating that the GBM has intrinsic permselectivity properties. Compared to *LAMB2* nulls, most human *LAMB2* missense mutations affect the LN domain[21] and are less severe; they are categorized as nephrotic syndrome type 5 (NPHS5, OMIM 614199) and encompass a wide spectrum of sub-Pierson phenotypes.[21] Because the LN domain mediates laminin polymerization, LAMB2 LN domain missense mutations potentially inhibit laminin polymerization, which is predicted to destabilize the GBM with a less direct effect on podocyte foot processes.

We previously characterized three human *LAMB2* missense mutations in mice, including two secretion-defective mutants (C321R and R246Q) that mimicked the patients’ strong phenotypes [22,23] and one incompletely polymerization-defective mutant (S80R).[24] The S80R mutation (S83R in mouse) failed to produce even modest proteinuria and exhibited an incomplete polymerization defect in vitro, despite progressive nephrotic syndrome in the

human.[21,25] Although *Lamb2*$^{S83R/S83R}$ mice showed no phenotype, *Lamb2*$^{+/S83R}$ heterozygosity dramatically exacerbated the Alport phenotype,[24] indicating that S83/S80 is important for GBM stability and that a more severe laminin polymerization defect should affect filtration more significantly. Serendipitously, the CRISPR strategy used to generate the *Lamb2*^{S83R} mutant mouse also generated a *Lamb2* deletion mutant lacking 44 amino acids in the polymerizing LN domain, leading to a new genetic model of nephrotic syndrome induced by defective laminin polymerization.

RESULTS

Lamb2-Del44 (Del44) founders were identified by the presence of a 219 bp shift in the genomic DNA PCR product (Figure 1A) from a CRISPR/Cas9 gene editing experiment designed to produce the *Lamb2*-S83R point mutation.[24] Sequencing of the PCR product revealed deletion of intron 3 and parts of exons 3 and 4, resulting in an in-frame exon fusion (Figure 1B, Supplementary Figure S1) and a predicted 44 amino-acid loss spanning mouse LAMB2-P76-A119 (Figure 1). A homology fit to the LAMB1 LN-LEa4 crystal structure[26] was obtained for LAMB2 with HHpred software and rendered into a ribbon diagram with PyMOL (Figures 1C and 1D). Based on the LAMB1 LN crystal structure, the Del44 sequence (red) comprises the majority of a structurally low-ordered segment that is external to a central β-sandwich core.[26] The segment includes the human S80R/murine S83R mutation (purple) that we previously characterized,[24,26] and a potential internal disulphide bond between two cysteines (C80-C91, yellow) near a β-hairpin turn at the top of the LN domain. The loss of the potential C80-C91 disulphide bond is unlikely to perturb the remaining LN domain structural integrity.

The Del44 sequence begins 3 amino acids after C71, which is predicted to bind C94 within the deleted sequence (Figure 1D)[26] and would not likely be disulphide bonded in LAMB2-Del44, allowing for potential secretion and stability defects. The bonding status of these cysteines and influence on protein folding, secretion, and/or stability remain untested. The Del44 sequence resides between the 1st and 2nd β-sheets of the β-sandwich core, and therefore its loss could lead to disorder within the β-sandwich core. However, due to the predicted organization and low secondary structure of the segments preceding and following the deleted 44 amino acids, it may be possible that enough sequence remains between the 1st and 2nd β-sheets to bridge the space and allow normal organization of the β-sandwich core. The degree to which loss of the 44 amino acids influences overall LN domain architecture, stability, or intracellular protein processing are undetermined here.

In an established in vitro assay, laminin polymerization mediates laminin retention on Schwann cells via receptors in the cell membrane.[24,27-30] Our previous investigation of LAMB2-S83R indicated ~50% reduction in retention of LM-121 heterotrimers containing LAMB2-S83R on Schwann cells relative to wild-type LM-121. [24] The location of S83R within the Del44 deleted sequence predicts further impairment of laminin polymerization of LM-121 containing LAMB2-Del44. Consistent with this hypothesis, Del44 LM-121 heterotrimers exhibited greater than 90% reduced polymerization compared to wild-type LM-121 at 28 nM laminin (Figure 2A & 2B). *Lamb2*$^{S83R/S83R}$ mice lacked a phenotype, but S83R heterozygotes dramatically exacerbated the Alport syndrome phenotype.[24] We

therefore tested additionally whether multiple molecular interactions, such as within the GBM, might help to stabilize polymerization-defective LAMB2 mutants. The inclusion of collagen IV and nidogen with laminin heterotrimers significantly increased Schwann cell retention of LAMB2-S83R and LAMB2-Del44 mutant LM-121, and, surprisingly, also enhanced wild-type LM-121 (Figure 2A and 2B). Collectively these data suggest that multiple molecular interactions promote retention of polymerization-defective laminins in the GBM. Cell-free polymerization assays, in which polymerized laminins are separated from remaining monomeric laminin heterotrimers via centrifugation, demonstrated trends toward polymerization defects similar to the Schwann cell assays, with a more robust defect for LAMB2-Del44 (Supplementary Figure S2).

Elevated urinary albumin:creatinine ratios (ACR) were detected in Del44 mice by ELISA (Figure 3A; $\log_{10}$ of ACRs are shown in mg/g to better visualize control data points) and SDS-PAGE (Figure 3B) after the first month. ACRs progressively increased between 1-2 months of age and plateaued between 3-6 months at ~200,000 mg/g average; ACR of some samples ranged from ~350,000 - 460,000 mg/g. 24-hour urine collection revealed polyuria in Del44 mice by 3 months (Figure 3C). Confocal immunofluorescence imaging revealed reduced quantity and diffuse localization of aquaporin-2 in many cortical tubules (Supplementary Figure S3), suggesting that nephron dysfunction promotes polyuria in part through aquaporin-2 dysregulation. Although some Del44 mice died spontaneously between 2-13 months of age with an average lifespan of 6.8 months (Figure 4A), 7 Del44 mice euthanized between 11 and 15 months of age (data not shown) may have lived even longer and indicate that the actual average lifespan is higher. Despite heavy proteinuria at 3.7 months, average blood urea nitrogen (BUN) only increased modestly to 40-50 mg/dL after 6 months of age (Figure 4B). Plasma sampled from two mice within one week of end stage renal disease during the 9th month of age revealed sudden spikes in BUN (70 mg/dL and 113 mg/dL; see error bar at 9 months, Figure 4B), suggesting that the slow reduction in renal function in Del44 mice can suddenly advance to ESRD.

Hypoalbuminemia (Figure 4C), elevated blood cholesterol (Figure 4D), and consistent observation of peritoneal fluid at euthanasia (not shown) completed the spectrum of nephrotic syndrome by 3 months of age. In addition to renal failure, *Lamb2*$^{-/-}$ mice also display neuromuscular junction defects.[31] Although the gross motor defects observed in *Lamb2*$^{-/-}$ mice (hind-limb retraction) were not observed in Del44 mice, neurofilament-M, synaptic vesicle glycoprotein 2, and acetylcholine receptor staining revealed neuromuscular junction fragmentation, sometimes in combination with axon swelling, within the Del44 diaphragm muscle (Supplementary Figure S4).

Renal histopathology was assessed in Del44 kidneys by PAS histochemistry (Figure 5). Despite the presence of significant proteinuria between 1-2 months of age (5-8 weeks), tubular dilations, protein casts, and diminished staining of proximal tubule brush borders were not evident until 2 months (9 weeks). At 3-4 months (15 weeks), when albuminuria peaked (Figure 3A), dilations and protein casts were increased but with only GBM thickening and no observable interstitial fibrosis (Figure 5). Finally, 8-9 month (37 weeks) old kidneys consistently exhibited increased numbers of tubular protein casts and dilations,

glomerulosclerosis (FSGS, diffuse mesangial sclerosis, global sclerosis), and interstitial infiltrates and fibrosis (Figure 5).

Podocyte foot process effacement is a hallmark of proteinuria. We previously demonstrated that proteinuria precedes foot process effacement in *Lamb2−/−* mice.[20] To assess podocyte morphology we performed transmission electron microscopy at time points up to ~3 months (15 weeks) and determined the number of foot processes per micrometer of GBM in Del44 (Figure 6A and 6D) and control mice (Figure 6E). At proteinuria onset (5 weeks), Del44 foot processes were slightly wider than control on average (Figure 6A vs. 6E, & 6F). From 1-2 months of age (6-9 weeks) foot process widening increased with maintenance of slit diaphragms (Figure 6B, 6C, & 6F). At 3 months of age (15 weeks) foot processes exhibited widespread but surprisingly incomplete effacement (Figure 6D), given the degree of albuminuria and nephrotic syndrome sequelae observed at this age (Figures 3 and 4).

Podocyte expression of the intermediate filament protein desmin is considered a marker of podocyte injury.[32] We observed desmin in podocytes as early as 1 month of age (Figure 7A), indicating podocyte abnormalities prior to overt albuminuria, and even higher desmin levels by 3 months (Supplementary Figure S5A). Nephrin and podocin exhibited continuous staining, intensity, and co-localization near the GBM until 3 months of age, at which time only modest discontinuity and loss of intensity were observed (Figure 7B). By 8 months both nephrin and podocin staining were dramatically reduced and punctate (Supplementary Figure S5B). Synaptopodin expression remained robust in the Del44 GBM through 3 months of age (Supplementary Figure S5C), but at 8 months exhibited a modestly punctate pattern with fluorescence intensity comparable to WT (Figure 7C). We interpret the delayed effacement and maintenance of podocyte marker intensity and localization in Del44 mice as indications that the observed albuminuria, at least at initial stages, can be attributed to a defect in GBM permselectivity.

To determine if the Del44 deletion influences LAMB2 protein quantity and/or localization in the GBM, we evaluated LAMB2 by immunostaining via confocal microscopy. In line with modulation of polymerization by collagen IV and nidogen (Figure 2A and 2B), the quantity of LAMB2-Del44 exhibited an average 30% reduction in the GBM at 1 month and 3 months of age (Figure 8A and 8B, Supplementary Figure S6A and S6B) despite a ~90% reduction in polymerization on Schwann cells in vitro (Figure 2A and 2B). In *Lamb2−/−* mice, the GBMs exhibit ectopic deposition of laminins, including LAMB1, LAMA1, and LAMA2, which are thought to insufficiently compensate for total LAMB2 loss.[20] LAMB1 (Figure 9A) and LAMA1 (Figure 9B) co-localized with nidogen in Del44 capillary loop GBMs as early as 1 month, preceding overt proteinuria. Although LAMB1 persisted in the GBM through 8 months of age (Supplementary Figure S7A and S7B), LAMA1 deposition appeared to become attenuated, exhibiting segmental GBM localization after 1 month of age (Supplementary Figure S7C and S7D). Only segmental LAMA2 (Figure 9C) and COL4A1 (Figure 9C) deposition were observed in Del44 capillary loops at 8 months of age. While deposition of LAMB1 in the LAMB2-deficient GBM fails to compensate for total LAMB2 loss, robust deposition of LAMB1 in Del44 GBM before proteinuria and in the absence of additional aberrant laminins or collagen IV suggests that LAMB1 may initially compensate for the 30% loss of LAMB2-Del44.

DISCUSSION

We have been investigating the pathogenic mechanisms of human *LAMB2* missense mutations using mouse models in order to determine what therapies might be effective. The current work describes a novel, serendipitous mouse *Lamb2* deletion mutation leading to a chronic nephrotic syndrome with 1) an unusually long lifespan; 2) delayed foot process effacement; and 3) delayed fibrosis. LAMB2-Del44 lacks 44 amino acids located within the LN domain that is critical for laminin polymerization (Figure 1).[28,33] The LAMB2-S83R (S80R in humans) and Del44 mutations exhibited ~50% and ~90% reduced polymerization, respectively, in a cell-based polymerization assay (Figure 2, Supplementary Figure S2). Whereas the S83R mouse required a second hit to produce a phenotype in mice,[24] Del44 mice spontaneously developed albuminuria in the 1st month (Figure 3) and nephrotic syndrome between 2-3 months (Figure 4). Most Del44 mice exhibited heavy proteinuria and onset of nephrotic syndrome by 3 months with neither significant glomerular nor interstitial fibrosis, and many endured these sequelae for up to 8 months with only a mild functional decline. In this regard Del44 mice may represent patients with stable proteinuria but mild or no functional decline, a relationship that is poorly understood. Given these features, we consider the Del44 mouse to be an ideal model for the testing of nephrotic syndrome therapeutics.

Proteinuria has been strongly associated with progression to end stage renal disease, but the contribution of proteinuria to injury is incompletely understood. Many factors have been investigated in vitro as potential insults to podocytes and nephron epithelium, particularly albumin, immunoglobulins, lipids, and activated complement.[34,35] The argument for albumin-induced tubular injury is supported by a plethora of in vitro data and some in vivo data.[34,35] Albumin-null Alport mice exhibit approximately 50% delayed time to ESRD with delayed foot process effacement and tubular injury,[36] which strongly suggests that filtered albumin is a significant contributor to renal injury. In contrast, however, results from experiments in Nagase analbuminemic rats (NARs) suggested neither protection nor exacerbation by the lack of albumin after various glomerular injuries, including surgically-induced hypertension, puromycin aminonucleoside nephrosis, and adriamycin nephropathy.[37-39] Del44 mice exhibited almost no signs of fibrosis through progression of albuminuria to an averaged ACR peak of 200 g/g at 3.7 months (Figure 3). Notably, whereas the slowly progressing C57BL/6J and rapidly progressing 129X1/SvJ Alport models exhibit sharp increases in BUN and reach ESRD with significant albuminuria,[40] Del44 mice endured much higher albuminuria for up to another 4 months with only modest increases in BUN (Figures 3 and 4). Collectively the phenotypes of NARs, Alport mice, and LAMB2-Del44 mice indicate that albumin-induced injury per se might be minimal, but may add to or synergize with one or multiple etiological factors to exacerbate injury.

Understanding the mechanisms of glomerular filtration is critical for directing potential therapeutic strategies to limit proteinuria and reduce renal disease. Consistent observations of foot process effacement concomitant with or preceding proteinuria in abnormal podocytes (e.g. nephrin, podocin, and CD2AP mutants) and inflammatory injury models (e.g., nephrotoxic serum) promote a podocyte-centric mechanism of filtration, mediated by slit diaphragm integrity. However, both theory and evidence indicate that the GBM confers

permselectivity, though likely not entirely independent of podocytes.[20,41-43] *Lamb2−/−* mice exhibit proteinuria preceding effacement in the first 7 days of life,[20] suggesting that the GBM is intrinsically permselective. Throughout the 2nd month of life Del44 foot processes were widened, but they otherwise maintained the typical vertical foot process shape perpendicular to the GBM, with obvious slit diaphragms despite heavy proteinuria. Even after 3 months of age, despite ACRs ranging from 50-460 g/g and established nephrotic syndrome hallmarks, foot processes were widely but incompletely effaced.

Models of GBM dysfunction typically exhibit multiple indicators of podocyte injury and abnormal GBM composition prior to fibrosis. Only desmin (Figure 7) and ectopic laminin β1 (Figure 9) were robust and consistent in Del44 podocytes and GBM, respectively. Desmin and laminin β1 expression prior to proteinuria could signify increased protein in the ultrafiltrate, or an adaptive compensatory response by podocytes attached to the defective LAMB2-Del44 substrate. The collective lack of ectopic laminin localization (LAMA1, LAMA2) in the Del44 GBM that is typically found in Alport,[24,44,45] *Lamb2−/−*,[46] and *Cd151−/−* [44] GBMs, as well as remarkable preservation of nephrin, podocin, and synaptopodin expression up to 15 weeks of age, indicate that podocyte injury is limited in Del44 mice. Therefore, we conclude that the polymerization defect of LAMB2-Del44 promotes proteinuria through reduced GBM permselectivity.

Our characterizations of LAMB2 LN domain mutations (Refs.[22-24] and this report) demonstrate that determining the mechanism of dysfunction is critical for designing therapeutic strategies. Improvements in the *Lamb2−/−* phenotype by overexpression of secretion defective mutants (C321R, R246Q)[22,23] suggests that enhanced expression of the analogous human mutants in patients should provide therapeutic benefits, though it could also increase podocyte ER stress.[22,23,47,48] The mechanism of reduced LAMB2-Del44 quantity in the GBM was not investigated, leaving unsolved the possibility of decreased secretion, in which case overexpression should improve the Del44 phenotype. However, we note that in vitro data suggested that LAMB2-R246Q is both secretion- and polymerization-defective,[28] and might require some degree of both increased expression and polymerization for complete function. In line with this hypothesis, relatively high LAMB2-R246Q overexpression abrogated aberrant capillary loop GBM LAMB1 and podocyte desmin expression but did not completely prevent proteinuria.[22] The potential for rescue of polymerization-defective laminins has been demonstrated in vitro and in vivo with rationally designed laminin short arm-nidogen fusion proteins that rescue polymerization of laminin trimers missing either α, β, or γ chain LN domains.[28,49] Such polymerization-focused approaches should also be effective for LN domain missense mutations that hinder polymerization.

The pathogenic mechanisms of several LAMB2 LN domain missense mutations remain uncharacterized. The murine LAMB2-C185Y expressed in the *nephertiti* mouse was logically presumed to be moderately secretion-defective due to the cysteine mutation that may affect protein folding, but in vivo protein expression data for mechanistic insight are lacking.[50] This mouse mimics the delays in pathology, functional decline, and GBM abnormalities observed in Del44 mice, in contrast to the likely more severely secretion-

defective R246Q and C321R mutants.[22,23] If secretion-defective, then C185Y might also be rescued by enhanced expression similar to R246Q and C321R transgenic mice.[22,23]

Herein we have demonstrated that the LAMB2-Del44 mouse is a remarkably long-lived model of nephrotic syndrome that exhibits resistance to glomerulosclerosis, tubulointerstitial fibrosis, and functional decline at levels of proteinuria much higher than those associated with ESRD in other models, such as Alport syndrome. The Del44 mutant phenotype represents the first experimental evidence that a laminin polymerization defect on its own can cause proteinuria and ESRD. Moreover, the delayed foot process effacement observed in Del44 mice contributes to our understanding of filtration mechanisms by serving as additional evidence of the GBM's inherent permselectivity, which was initially observed in *Lamb2*$^{-/-}$ mice. Lastly, Del44 mice may serve as a tool for understanding slowly progressing human nephrotic syndrome and discovering new approaches to mitigating its various symptoms.

METHODS

Mice

All animal experiments conformed to the NIH Guide for the Care and Use of Laboratory Animals and were approved by the Washington University Institutional Animal Care and Use Committee. The CRISPR/Cas9 approach to generate the murine *Lamb2*^{S83R} knock-in allele was previously described.[24] The founder carrying the *Lamb2*^{Del44} mutation was mated with *Lamb2*$^{+/-}$ mice on a mixed B6CBA background[51] to produce *Lamb2*$^{-/Del44}$ compound heterozygotes and eventually *Lamb2*$^{Del44/Del44}$ homozygotes. Del44 mice exhibited no developmental defects and offspring showed the expected Mendelian inheritance. No phenotypic differences were observed between *Lamb2*$^{-/Del44}$ and *Lamb2*$^{Del44/Del44}$ mice (collectively, "Del44"), nor between *Lamb2* +/+, +/−, or +/Del44 mice (collectively, "controls"). The *Lamb2*^{Del44} allele was detected with the following PCR primers from *Lamb2*: Forward, 5'- GATGTACCTGGCTGTTCTCGAGGAAGCTGC -3'; reverse, 5'-GGACGTGACCATGCTTCACACATAGAGCAC-3'. The WT and mutant amplicons are 647 bp and 428 bp, respectively.

Urine and plasma analyses

Urine creatinine levels were determined with the Quantichrome creatinine detection kit. Some urine samples were collected in metabolic cages for 24-hours to assess urine output. Plasma and urinary albumin were determined with an anti-albumin sandwich ELISA kit (Bethyl). BUN was determined with the Quantichrome Urea detection kit. Total plasma cholesterol determination was performed by the Washington University Diabetes Models Phenotyping Core with a colorimetric total cholesterol detection kit (Infinity).

Microscopy

PAS staining of paraffin kidney sections and transmission electron microscopy were performed by standard methods. For immunofluorescence, kidneys were frozen in OCT and cryo-sectioned at 7μm. Primary antibodies were incubated on tissues in PBS containing 1% denatured bovine serum albumin overnight. Primary antibodies were rabbit anti-LAMB1 and

- LAMB2,[52] rabbit anti-LAMA1,[53] rat anti-LAMA2 (clone 4H8-2, Axxora), rabbit anti-LM-111 (Sigma), rat anti-COL4A1[54] (following urea/glycine denaturation),[15] goat anti-nephrin (AF3159, R&D), rabbit anti-podocin (p35),[55] mouse anti-synaptopodin (clone G1, a gift from Dr. Peter Mundel), mouse anti-desmin (clone D33, Dako), rat anti-nidogen (Clone ELM1, Santa Cruz), hamster anti-mouse agrin,[56] and goat anti-aquaporin2 (Santa Cruz). Secondary antibodies were incubated on sections in 1% denatured bovine serum albumin in PBS for one hour at room temperature. Whole mount immunofluorescence staining of diaphragms was performed following perfusion and overnight fixation in 4% paraformaldehyde with anti-neurofilament-M (2H3) and anti-vesicle glycoprotein 2 (Developmental Studies Hybridoma Bank) overnight at 4°C, and counterstained with Alexa 488 with Alexa 594-conjugated α-bungarotoxin to visualize acetylcholine receptors. Images were taken on a Nikon Eclipse 80i with an Olympus DP72 camera and Cellsens software, or on an Olympus IX81 Confocal microscope with Fluoview ver. 3.1b software.

DNA Constructs and Protein Production

Expression vectors for the mouse laminin α1 and human γ1 subunits were previously described.[30] Mouse laminin β2 pcDNA3.1Zeo was a generous gift from Takako Sasaki. An N-terminal Flag epitope was added using overlapping PCR. A 2342 bp secondary PCR product was digested and ligated into the mouse laminin β2 pcDNA vector. The S83R point mutation and the 44 amino acid deletion (121Del44) were also engineered into the mouse laminin β2 construct using overlapping PCR followed by digestion and ligation of secondary products into the pcDNA3.1Zeo construct. All laminin constructs were stably transfected into HEK293 cells and purified as previously described.[30] The nidogen-1 pCIS expression vector was a generous gift from Rupert Timpl. Nidogen-1 and collagen type IV were isolated as previously described[30,57] by metal chelating chromatography, and from lathyritic mouse EHS tumor and by salt fractionation and DEAE-cellulose chromatography,[58] respectively.

Laminin polymerization assays

Laminin polymerization on Schwann cells was performed as described.[24,30] Briefly, Schwann cells (SCs) were grown as described,[59] incubated at 37°C with recombinant laminins (9-36 nM), washed with PBS, and then fixed with 3% paraformaldehyde for 15 min at RT. Laminin was visualized by fluorescence with 1 μg/ml rabbit anti-laminin E3 and DAPI. Digital images were recorded from 6-7 fields/condition, each at 1300 × 1030 pixels. Fluorescence levels were estimated with ImageJ.[59] The summed intensities from each field were divided by the area followed by background subtraction and division by the number of counted nuclei. Data were expressed as the mean ± standard deviation of normalized net summed intensities/cell with plots and statistical calculations prepared in SigmaPlot 12.5 (Systat). Significance was determined by one-way ANOVA followed by Holm-Sidak pairwise comparisons.

Cell-free laminin polymerization was performed as described.[30] Briefly, purified laminins were incubated in a polymerization buffer (TBS, 1mM $CaCl_2$, 0.1% TritonX 100) at 0.2-0.8 mg/ml at 37°C in 0.5 ml Eppendorf tubes. Reactions were centrifuged at 11,000 x g. Supernatants and pelleted polymers were diluted into equal final volumes of SDS and

separated by SDS-PAGE. Gels were stained with Coomassie and the density of laminin α1 was quantified for both fractions in ImageJ software to determine the percentage of laminin α1 in the polymerized fraction.

Supplementary Material

Refer to Web version on PubMed Central for supplementary material.

ACKNOWLEDGMENTS

We thank Gloriosa Go and Jennifer Richardson for technical assistance; the Transgenic Vectors Core for design and validation of the CRISPR/Cas9 guide RNA; the Mouse Genetics Core for nucleic acid microinjections and mouse husbandry; the Pulmonary Morphology Core and Advanced Imaging and Tissue Analysis Core (supported by NIH P30DK052574) for histology; the Diabetes Research Center Diabetes Models Phenotype Core (supported by NIH P30DK020579) for plasma cholesterol assays; and the Washington University Center for Cellular Imaging for electron microscopy. We are grateful to Takako Sasaki for the mouse laminin β2 pcDNA3.1 Zeocin expression construct and to Peter Mundel and Dorin-Bogdan Borza for gifts of antibodies.

This work was funded by NIH grants R01DK078314 and R01DK058366 to JHM, R01DK036425 to PDY, and grants R01NS078214 and R01AG051470 to HN. SDF was supported by NIH T32DK007126. Production of knock-in mice was supported by the Diabetes Research Center Transgenic and ES Cell Core (P30DK020579) and the Digestive Diseases Research Core Center Murine Models Core (P30DK052574).

REFERENCES

1. Miner JH. The glomerular basement membrane. Exp Cell Res. 2012;318:973–978. [PubMed: 22410250]
2. Abrahamson DR. Origin of the glomerular basement membrane visualized after in vivo labeling of laminin in newborn rat kidneys. J Cell Biol. 1985;100:1988–2000. [PubMed: 3889015]
3. St John PL, Abrahamson DR. Glomerular endothelial cells and podocytes jointly synthesize laminin-1 and -11 chains. Kidney Int. 2001;60:1037–1046. [PubMed: 11532098]
4. Reiser J, Kriz W, Kretzler M et al. The glomerular slit diaphragm is a modified adherens junction. J Am Soc Nephrol. 2000;11:1–8. [PubMed: 10616834]
5. Simic I, Tabatabaeifar M, Schaefer F. Animal models of nephrotic syndrome. Pediatr Nephrol. 2013;28:2079–2088. [PubMed: 23250714]
6. Wang CS, Greenbaum LA. Nephrotic Syndrome. Pediatr Clin North Am. 2019;66:73–85. [PubMed: 30454752]
7. Gross O, Licht C, Anders HJ et al. Early angiotensin-converting enzyme inhibition in Alport syndrome delays renal failure and improves life expectancy. Kidney Int. 2012;81:494–501. [PubMed: 22166847]
8. Greka A, Mundel P. Cell biology and pathology of podocytes. Annu Rev Physiol. 2012;74:299–323. [PubMed: 22054238]
9. Funk SD, Lin MH, Miner JH. Alport syndrome and Pierson syndrome: Diseases of the glomerular basement membrane. Matrix Biol. 2018;71-72:250–261. [PubMed: 29673759]
10. Pozzi A, Yurchenco PD, Iozzo RV. The nature and biology of basement membranes. Matrix Biol. 2017;57–58:1–11.
11. Yurchenco PD. Integrating Activities of Laminins that Drive Basement Membrane Assembly and Function. Curr Top Membr. 2015;76:1–30. [PubMed: 26610910]
12. Yurchenco PD, Cheng YS. Self-assembly and calcium-binding sites in laminin. A three-arm interaction model. J Biol Chem. 1993;268:17286–17299. [PubMed: 8349613]
13. Miner JH. Developmental biology of glomerular basement membrane components. Curr Opin Nephrol Hypertens. 1998;7:13–19. [PubMed: 9442357]

14. Miner JH, Patton BL, Lentz SI et al. The laminin alpha chains: expression, developmental transitions, and chromosomal locations of alpha1–5, identification of heterotrimeric laminins 8-11, and cloning of a novel alpha3 isoform. J Cell Biol. 1997;137:685–701. [PubMed: 9151674]
15. Miner JH, Sanes JR. Collagen IV alpha 3, alpha 4, and alpha 5 chains in rodent basal laminae: sequence, distribution, association with laminins, and developmental switches. J Cell Biol. 1994;127:879–891. [PubMed: 7962065]
16. Noakes PG, Miner JH, Gautam M et al. The renal glomerulus of mice lacking s-laminin/laminin beta 2: nephrosis despite molecular compensation by laminin beta 1. Nat Genet. 1995;10:400–406. [PubMed: 7670489]
17. Zenker M, Aigner T, Wendler O et al. Human laminin beta2 deficiency causes congenital nephrosis with mesangial sclerosis and distinct eye abnormalities. Hum Mol Genet. 2004;13:2625–2632. [PubMed: 15367484]
18. Zenker M, Tralau T, Lennert T et al. Congenital nephrosis, mesangial sclerosis, and distinct eye abnormalities with microcoria: an autosomal recessive syndrome. Am J Med Genet A. 2004;130A:138–145. [PubMed: 15372515]
19. Noakes PG, Gautam M, Mudd J et al. Aberrant differentiation of neuromuscular junctions in mice lacking s-laminin/laminin beta 2. Nature. 1995;374:258–262. [PubMed: 7885444]
20. Jarad G, Cunningham J, Shaw AS et al. Proteinuria precedes podocyte abnormalities in Lamb2−/− mice, implicating the glomerular basement membrane as an albumin barrier. J Clin Invest. 2006;116:2272–2279. [PubMed: 16886065]
21. Matejas V, Hinkes B, Alkandari F et al. Mutations in the human laminin beta2 (LAMB2) gene and the associated phenotypic spectrum. Hum Mutat. 2010;31:992–1002. [PubMed: 20556798]
22. Chen YM, Kikkawa Y, Miner JH. A missense LAMB2 mutation causes congenital nephrotic syndrome by impairing laminin secretion. J Am Soc Nephrol. 2011;22:849–858. [PubMed: 21511833]
23. Chen YM, Zhou Y, Go G et al. Laminin beta2 gene missense mutation produces endoplasmic reticulum stress in podocytes. Journal of the American Society of Nephrology. 2013;24:1223–1233. [PubMed: 23723427]
24. Funk SD, Bayer RH, Malone AF et al. Pathogenicity of a Human Laminin beta2 Mutation Revealed in Models of Alport Syndrome. J Am Soc Nephrol. 2018;29:949–960. [PubMed: 29263159]
25. Lehnhardt A, Lama A, Amann K et al. Pierson syndrome in an adolescent girl with nephrotic range proteinuria but a normal GFR. Pediatr Nephrol. 2012;27:865–868. [PubMed: 22228401]
26. Carafoli F, Hussain SA, Hohenester E. Crystal structures of the network-forming short-arm tips of the laminin beta1 and gamma1 chains. PLoS ONE. 2012;7:e42473. [PubMed: 22860131]
27. Li S, Liquari P, McKee KK et al. Laminin-sulfatide binding initiates basement membrane assembly and enables receptor signaling in Schwann cells and fibroblasts. J Cell Biol. 2005;169:179–189. [PubMed: 15824137]
28. McKee KK, Aleksandrova M, Yurchenco PD. Chimeric protein identification of dystrophic, Pierson and other laminin polymerization residues. Matrix Biol. 2018;67:32–46. [PubMed: 29408412]
29. McKee KK, Capizzi S, Yurchenco PD. Scaffold-forming and Adhesive Contributions of Synthetic Laminin-binding Proteins to Basement Membrane Assembly. J Biol Chem. 2009;284:8984–8994. [PubMed: 19189961]
30. McKee KK, Harrison D, Capizzi S et al. Role of laminin terminal globular domains in basement membrane assembly. J Biol Chem. 2007;282:21437–21447. [PubMed: 17517882]
31. Miner JH, Go G, Cunningham J et al. Transgenic isolation of skeletal muscle and kidney defects in laminin beta2 mutant mice: implications for Pierson syndrome. Development. 2006;133:967–975. [PubMed: 16452099]
32. Yaoita E, Kawasaki K, Yamamoto T et al. Variable expression of desmin in rat glomerular epithelial cells. Am J Pathol. 1990;136:899–908. [PubMed: 2183627]
33. Purvis A, Hohenester E. Laminin network formation studied by reconstitution of ternary nodes in solution. J Biol Chem. 2012;287:44270–44277. [PubMed: 23166322]

34. Zandi-Nejad K, Eddy AA, Glassock RJ et al. Why is proteinuria an ominous biomarker of progressive kidney disease? Kidney Int Suppl. 2004:S76–89. [PubMed: 15485426]
35. Abbate M, Zoja C, Remuzzi G. How does proteinuria cause progressive renal damage? J Am Soc Nephrol. 2006;17:2974–2984. [PubMed: 17035611]
36. Jarad G, Knutsen RH, Mecham RP et al. Albumin contributes to kidney disease progression in Alport syndrome. Am J Physiol Renal Physiol. 2016;311:F120–130. [PubMed: 27147675]
37. Abe H, Shibuya T, Odashima S et al. Alterations in the glomerulus in aminonucleoside nephrosis in analbuminemic rats. Nephron. 1988;50:351–355. [PubMed: 3237275]
38. Fujihara CK, Limongi DM, Falzone R et al. Pathogenesis of glomerular sclerosis in subtotally nephrectomized analbuminemic rats. Am J Physiol. 1991;261:F256–264. [PubMed: 1877649]
39. Okuda S, Oochi N, Wakisaka M et al. Albuminuria is not an aggravating factor in experimental focal glomerulosclerosis and hyalinosis. J Lab Clin Med. 1992;119:245–253. [PubMed: 1371800]
40. Andrews KL, Mudd JL, Li C et al. Quantitative trait loci influence renal disease progression in a mouse model of Alport syndrome. Am J Pathol. 2002;160:721–730. [PubMed: 11839593]
41. Fissell WH, Miner JH. What Is the Glomerular Ultrafiltration Barrier? J Am Soc Nephrol. 2018;29:2262–2264. [PubMed: 30030419]
42. Smithies O Why the kidney glomerulus does not clog: a gel permeation/diffusion hypothesis of renal function. Proc Natl Acad Sci U S A. 2003;100:4108–4113. [PubMed: 12655073]
43. Robinson GB, Walton HA. Glomerular basement membrane as a compressible ultrafilter. Microvasc Res. 1989;38:36–48. [PubMed: 2761432]
44. Delimont D, Dufek BM, Meehan DT et al. Laminin alpha2-mediated focal adhesion kinase activation triggers Alport glomerular pathogenesis. PLoS ONE. 2014;9:e99083. [PubMed: 24915008]
45. Kashtan CE, Kim Y, Lees GE et al. Abnormal glomerular basement membrane laminins in murine, canine, and human Alport syndrome: aberrant laminin alpha2 deposition is species independent. J Am Soc Nephrol. 2001;12:252–260. [PubMed: 11158215]
46. Suh JH, Jarad G, VanDeVoorde RG et al. Forced expression of laminin beta1 in podocytes prevents nephrotic syndrome in mice lacking laminin beta2, a model for Pierson syndrome. Proc Natl Acad Sci U S A. 2011;108:15348–15353. [PubMed: 21876163]
47. Kim Y, Lee H, Manson SR et al. Mesencephalic Astrocyte-Derived Neurotrophic Factor as a Urine Biomarker for Endoplasmic Reticulum Stress-Related Kidney Diseases. J Am Soc Nephrol. 2016;27:2974–2982. [PubMed: 26940092]
48. Kim Y, Park SJ, Manson SR et al. Elevated urinary CRELD2 is associated with endoplasmic reticulum stress-mediated kidney disease. JCI Insight. 2017;2.
49. McKee KK, Crosson SC, Meinen S et al. Chimeric protein repair of laminin polymerization ameliorates muscular dystrophy phenotype. J Clin Invest. 2017;127:1075–1089. [PubMed: 28218617]
50. Bull KR, Mason T, Rimmer AJ et al. Next-generation sequencing to dissect hereditary nephrotic syndrome in mice identifies a hypomorphic mutation in Lamb2 and models Pierson's syndrome. J Pathol. 2014;233:18–26. [PubMed: 24293254]
51. Noakes PG, Gautam M, Mudd J et al. Aberrant differentiation of neuromuscular junctions in mice lacking s-laminin/laminin beta2. Nature. 1995;374:258–262. [PubMed: 7885444]
52. Sasaki T, Mann K, Miner JH et al. Domain IV of mouse laminin beta1 and beta2 chains: structure, glycosaminoglycan modification and immunochemical analysis of tissue contents. European Journal of Biochemistry. 2002;269:431–442. [PubMed: 11856301]
53. Sasaki T, Giltay R, Talts U et al. Expression and distribution of laminin alpha1 and alpha2 chains in embryonic and adult mouse tissues: an immunochemical approach. Exp Cell Res. 2002;275:185–199. [PubMed: 11969289]
54. Ninomiya Y, Kagawa M, Iyama K et al. Differential expression of two basement membrane collagen genes, COL4A6 and COL4A5, demonstrated by immunofluorescence staining using peptide-specific monoclonal antibodies. J Cell Biol. 1995;130:1219–1229. [PubMed: 7657706]
55. Roselli S, Gribouval O, Boute N et al. Podocin localizes in the kidney to the slit diaphragm area. Am J Pathol. 2002;160:131–139. [PubMed: 11786407]

56. Harvey SJ, Jarad G, Cunningham J et al. Disruption of glomerular basement membrane charge through podocyte-specific mutation of agrin does not alter glomerular permselectivity. American Journal of Pathology. 2007;171:139–152. [PubMed: 17591961]

57. Fox JW, Mayer U, Nischt R et al. Recombinant nidogen consists of three globular domains and mediates binding of laminin to collagen type IV. EMBO J. 1991;10:3137–3146. [PubMed: 1717261]

58. Yurchenco PD, Furthmayr H. Self-assembly of basement membrane collagen. Biochemistry. 1984;23:1839–1850. [PubMed: 6722126]

59. McKee KK, Harrison D, Capizzi S et al. Role of laminin terminal globular domains in basement membrane assembly. Journal of Biological Chemistry. 2007;282:21437–21447. [PubMed: 17517882]

TRANSLATIONAL STATEMENT

Nephrotic syndrome is a condition caused by the massive, abnormal leak of blood albumin into the urine through the renal glomerulus, leading to low blood albumin (hypoalbuminemia), dramatically increased blood lipids (hyperlipidemia), and edema. No therapy exists for steroid resistant and refractory nephrotic syndromes, and the molecular mechanisms of injury by nephrotic syndrome sequelae are poorly understood. Many nephrotic patients maintain long-term albuminuria prior to ESRD and renal replacement therapy due to unknown causes; these patients are not currently represented by experimental models. Herein we describe a novel laminin β2 deletion mutant that exhibits heavy albuminuria that peaked prior to functional decline, significant glomerulosclerosis, and significant interstitial fibrosis. We predict that the *Lamb2*-Del44 mouse will serve as a useful model to study basic etiologies of nephrosis and potential therapies.

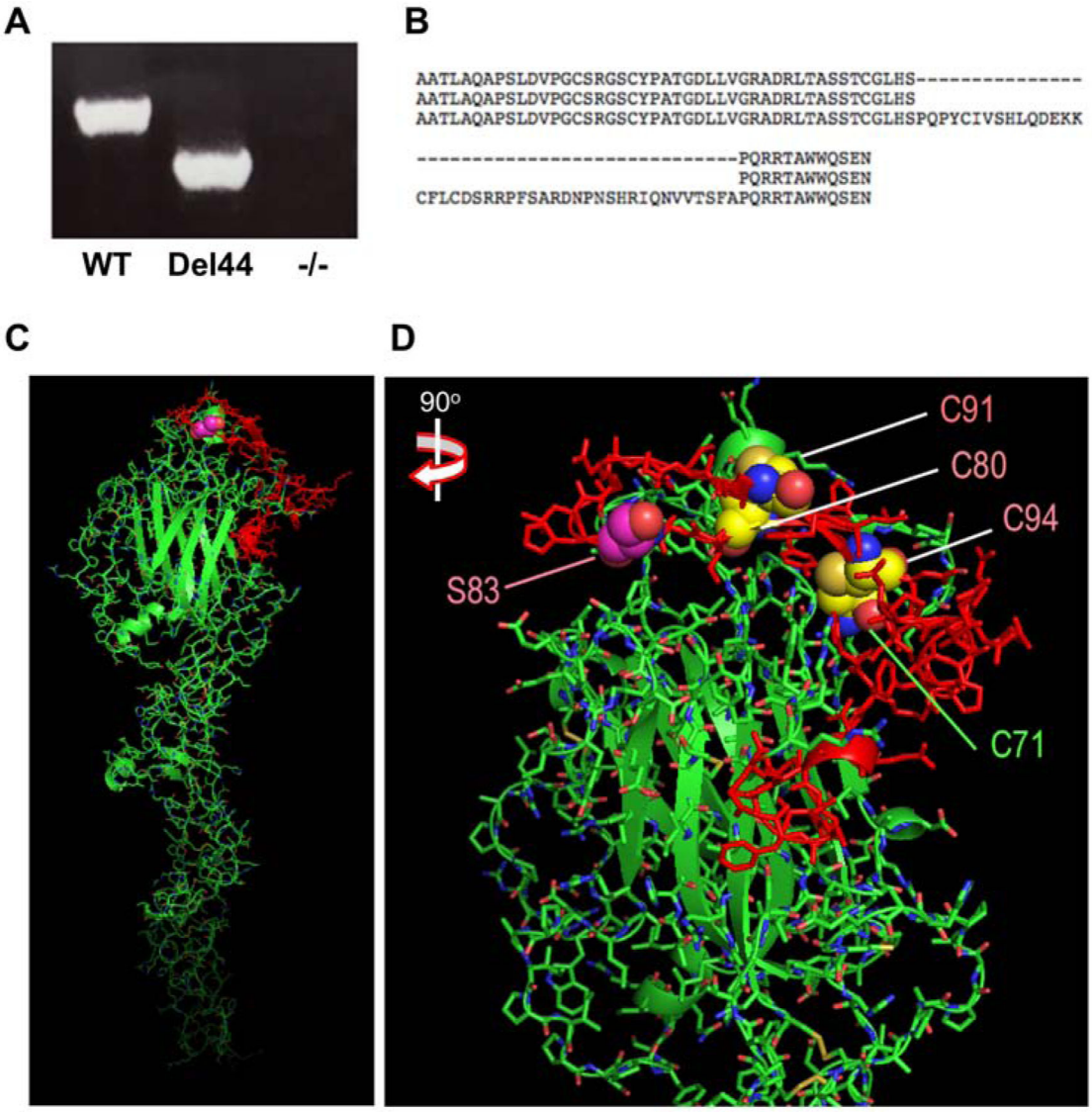

Figure 1. CRISPR/Cas9 gene editing induced a 44-amino acid deletion in the LAMB2 protein.

(a) PCR of genomic DNA using primers flanking the gRNA target/Cas9 cleavage site revealed a 219 bp shift in the product. **(b)** The deduced partial LAMB2 LN domain mutant protein sequence (top and middle rows) shows a 44-amino acid loss (hyphens) due to deletion of parts of exons 3 and 4, and intron 3. This 44-amino acid sequence includes S83 (CIV**S**HLQ). **(c)** A ribbon diagram of LAMB2 LN and LEa1 domains was rendered in PyMOL after a homology fit to LAMB1 in HHPred software. The Del44 sequence is shown in red, and S83 is shown as a space-filling molecule in purple. **(d)** A zoomed image of the LAMB2-Del44 ribbon diagram in (c) rotated 90° clockwise. In addition to a space-filling representation of S83 (purple), cysteines C80, C91, C94, and C71 are shown as space filling models in yellow. Red text for C80-C94 indicates their inclusion in the region deleted in Del44.

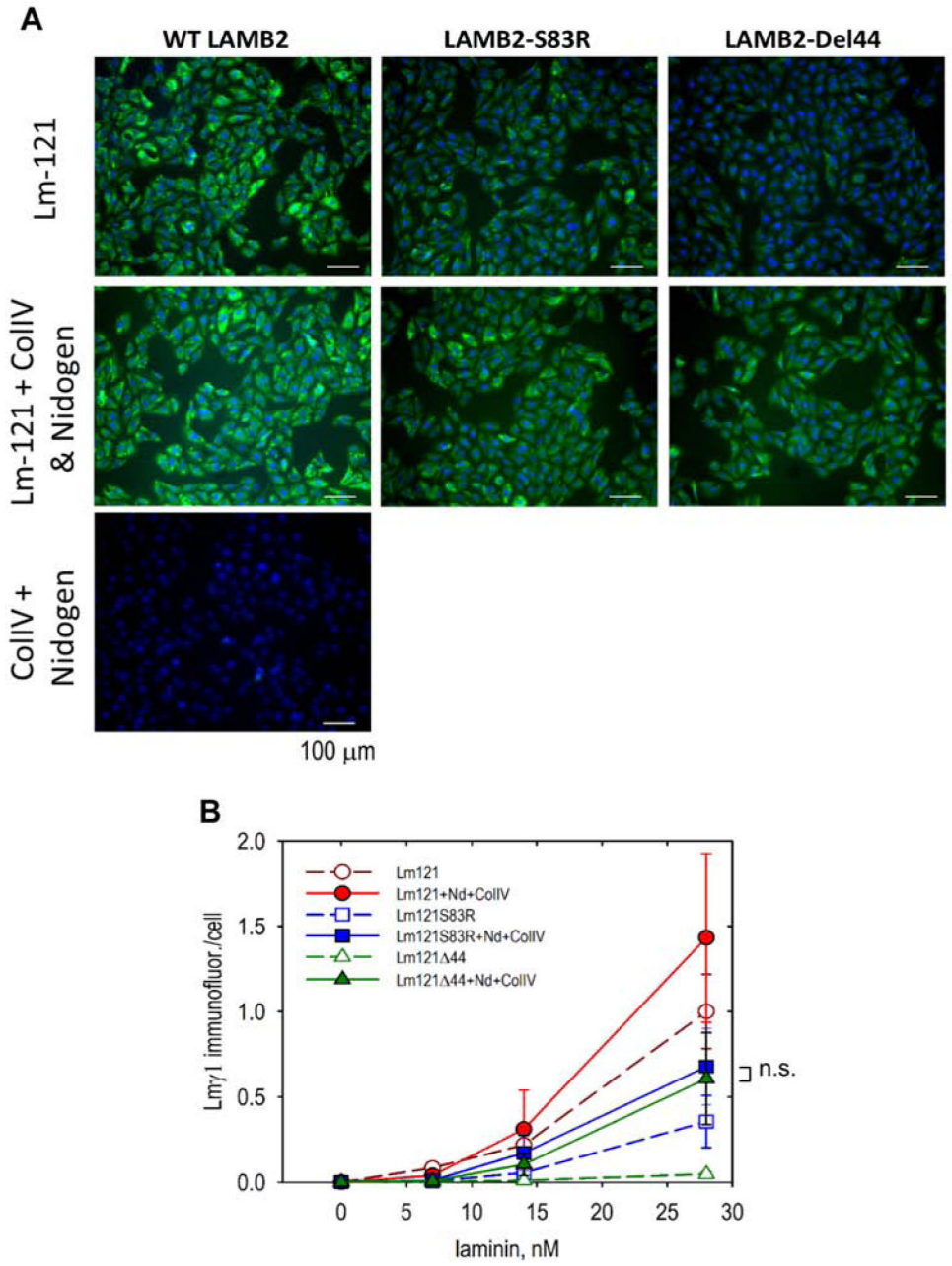

Figure 2. Defective polymerization of laminin containing LAMB2-S83R or -Del44 is modulated by multiple molecular interactions.

(a) Schwann cell cultures were incubated with wild-type, S83R, or Del44 laminin-121 (Lm-121) with or without the presence of collagen IV α1α1α2 (ColIV) and nidogen (Nd + ColIV), or only with collagen IV and nidogen. Laminin was visualized with anti-laminin E3 antibody and cells were stained with DAPI; n = 9-10 for each concentration and every condition. **(b)** Anti-laminin E3 immunofluorescence was normalized to DAPI for each condition. 2-way ANOVA followed by Holm-Sidak pairwise comparisons indicated significant concentration-dependent increases in polymerization (28nM vs 14nM and 7nM, $P < 0.05$) for wild-type and S83R laminins with and without nidogen and collagen IV,

excepting Del44 LM-121 by itself (--Δ--). All laminin conditions at 28nM were significantly different ($P < 0.003$), except for S83R LM-121 vs. Del44 LM-121 with nidogen and collagen IV, indicating polymerization defects in LAMB2 mutants and a stabilizing effect on LAMB2 mutant heterotrimers by nidogen + collagen IV.

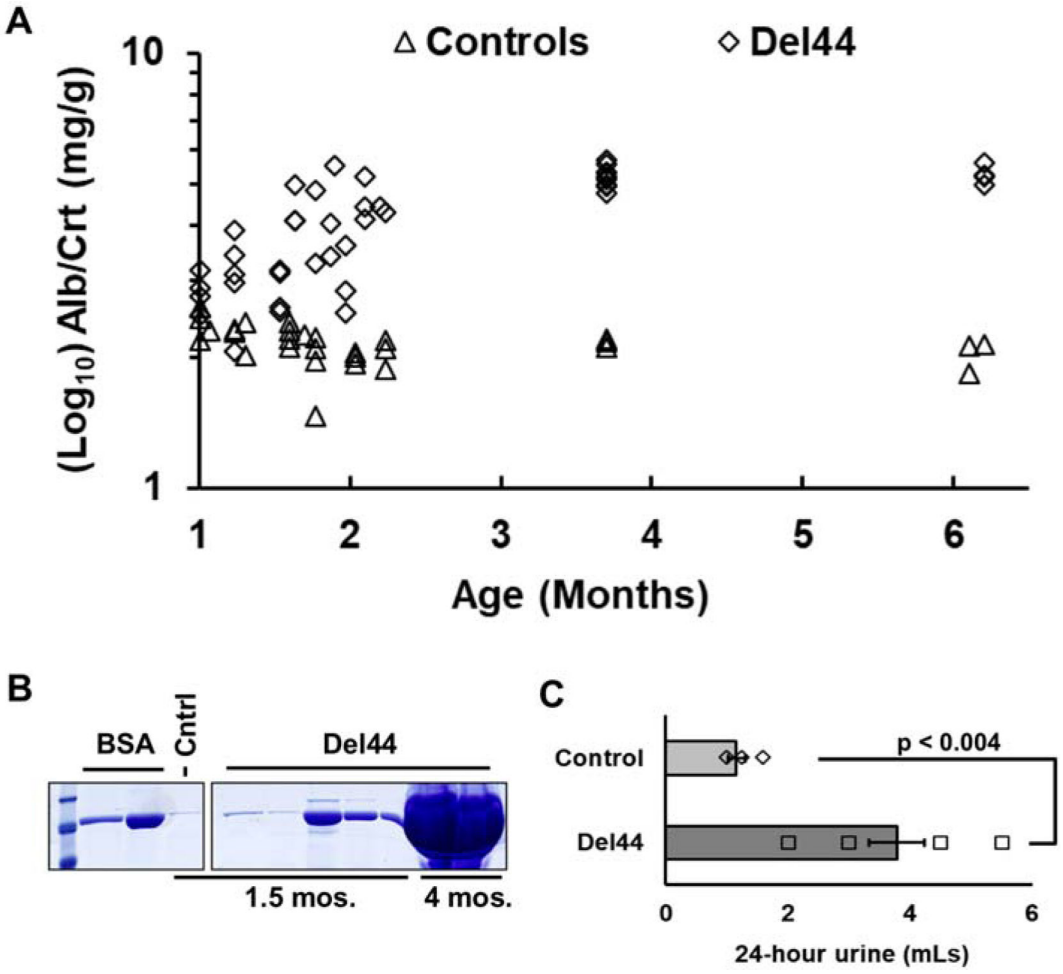

Figure 3. Urinalysis reveals a long-term, chronic proteinuria in Del44 mice.

(a) Urinary albumin was quantified by ELISA and normalized to urinary creatinine at the indicated time points; n = 3-5 for controls and 3-9 for Del44 mice. 2-way ANOVA revealed significant differences between Del44 and controls ($P < 0.05$). Tukey multiple pairwise comparison revealed an adjusted $P < 0.05$ between week 15 and weeks 4-7. **(b)** Representative creatinine-normalized urines collected at the indicated ages were run on an SDS-PAGE gel and stained with Coomassie to reveal urinary albumin. Cntrl = Control. **(c)** 24-hour urine collection from 3-month old control and Del44 mice indicated development of polyuria in Del44 mice. n = 4-6; $P < 0.004$ by Student's *t*-test.

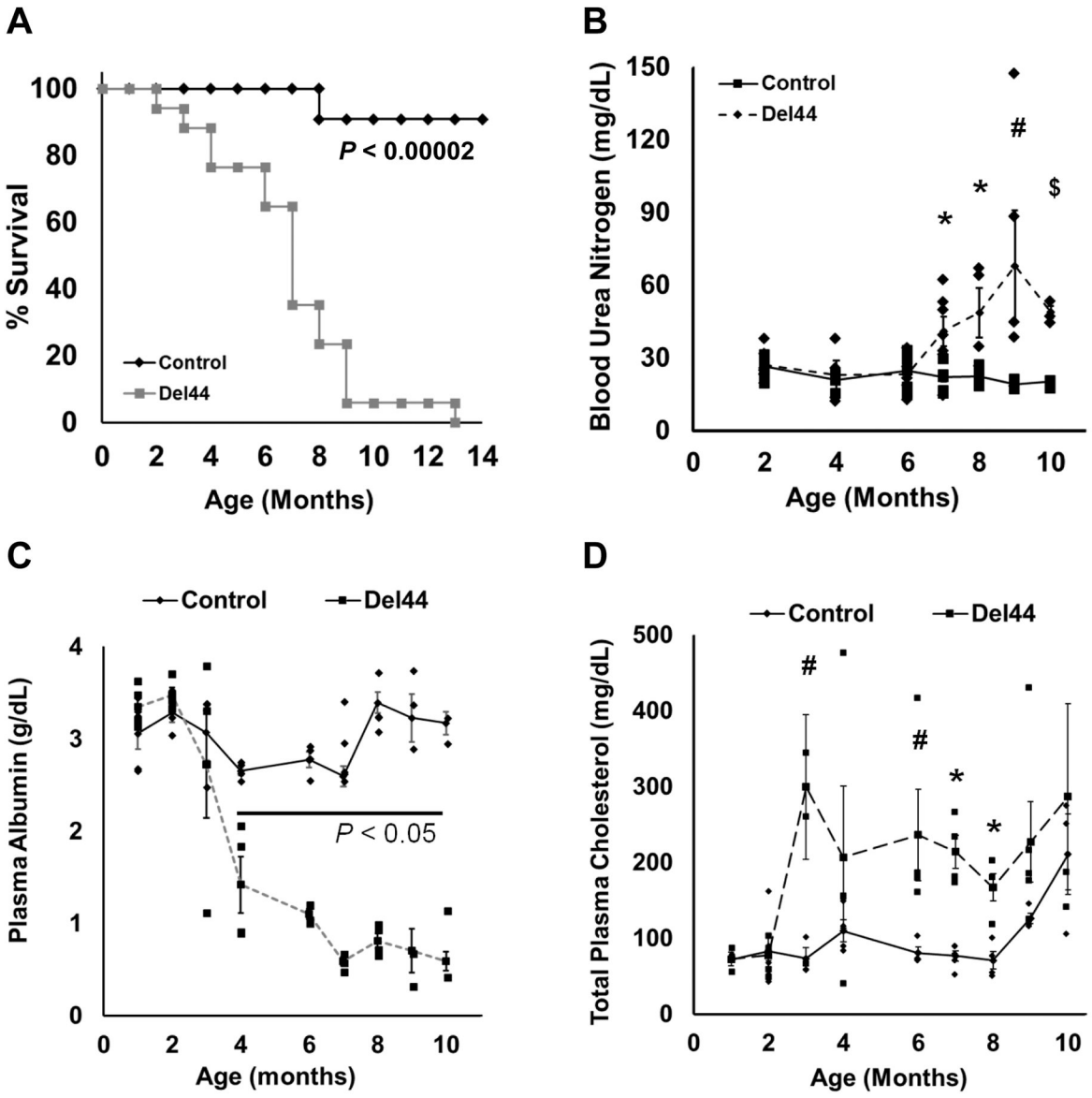

Figure 4. Survival and plasma analyses reveal features of nephrotic syndrome in Del44 mice.

(a) A log-rank survival analysis comparing control and Del44 littermates revealed significantly reduced viability in Del44 mice. n = 11 control and 15 Del44 mice. $P < 1.0 \times 10^{-5}$. **(b)** BUN levels in control and Del44 mice at the indicated ages revealed the onset of renal function decline at 7 months, which is delayed relative to proteinuria onset and plateau shown in Figure 3. n = 4-6; #, $P = 0.0505$; *, $P < 0.05$; $, $P < 0.01$. **(c)** Plasma albumin levels in control and Del44 mice revealed onset of hypoalbuminemia at 2-3 months of age. n = 3-5; *, $P < 0.001$. **(d)** Levels of plasma cholesterol indicated onset of hyperlipidemia in Del44 mice at 2-3 months. n = 3-5; *, $P < 0.05$ by Student's *t*-test.

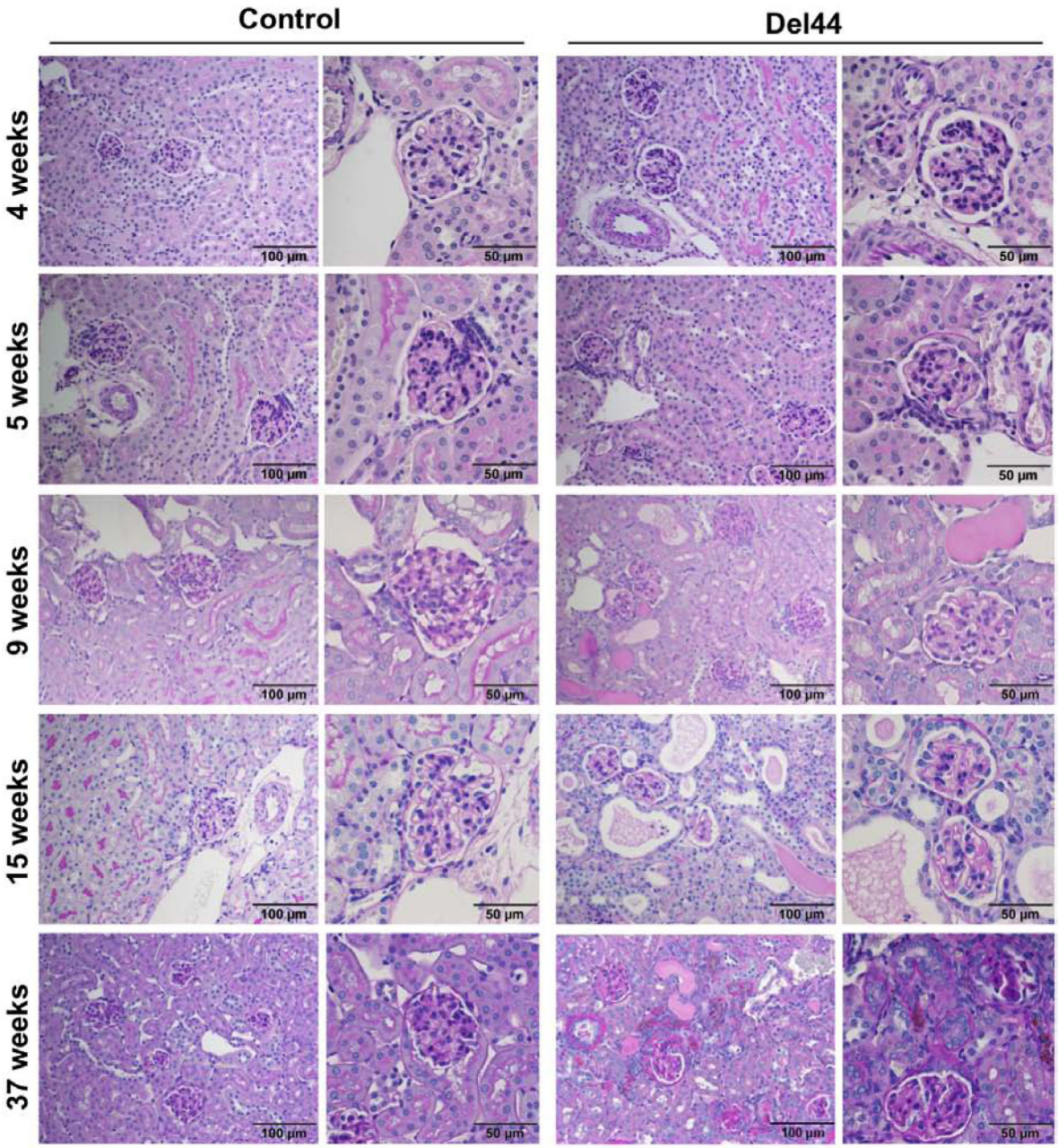

Figure 5. Periodic acid Schiff staining revealed delayed glomerular and interstitial fibrosis in Del44 mice.

Throughout the 2nd month of life (5-8 weeks of age) almost no pathology was observed in Del44 mice. Tubular dilations, protein casts, and reduced proximal tubule brush border staining were evident at 2 months of age (9 weeks). After 3.5 months (15 weeks) tubular dilations and protein casts were more frequent, and GBM thickening was pronounced. Between 8-9 months (37 weeks is shown) glomerulosclerosis was consistently observed, including global sclerosis and FSGS, with immune infiltrates and fibrosis evident throughout the interstitium. n = 3-5 per age group. Scale bars as indicated.

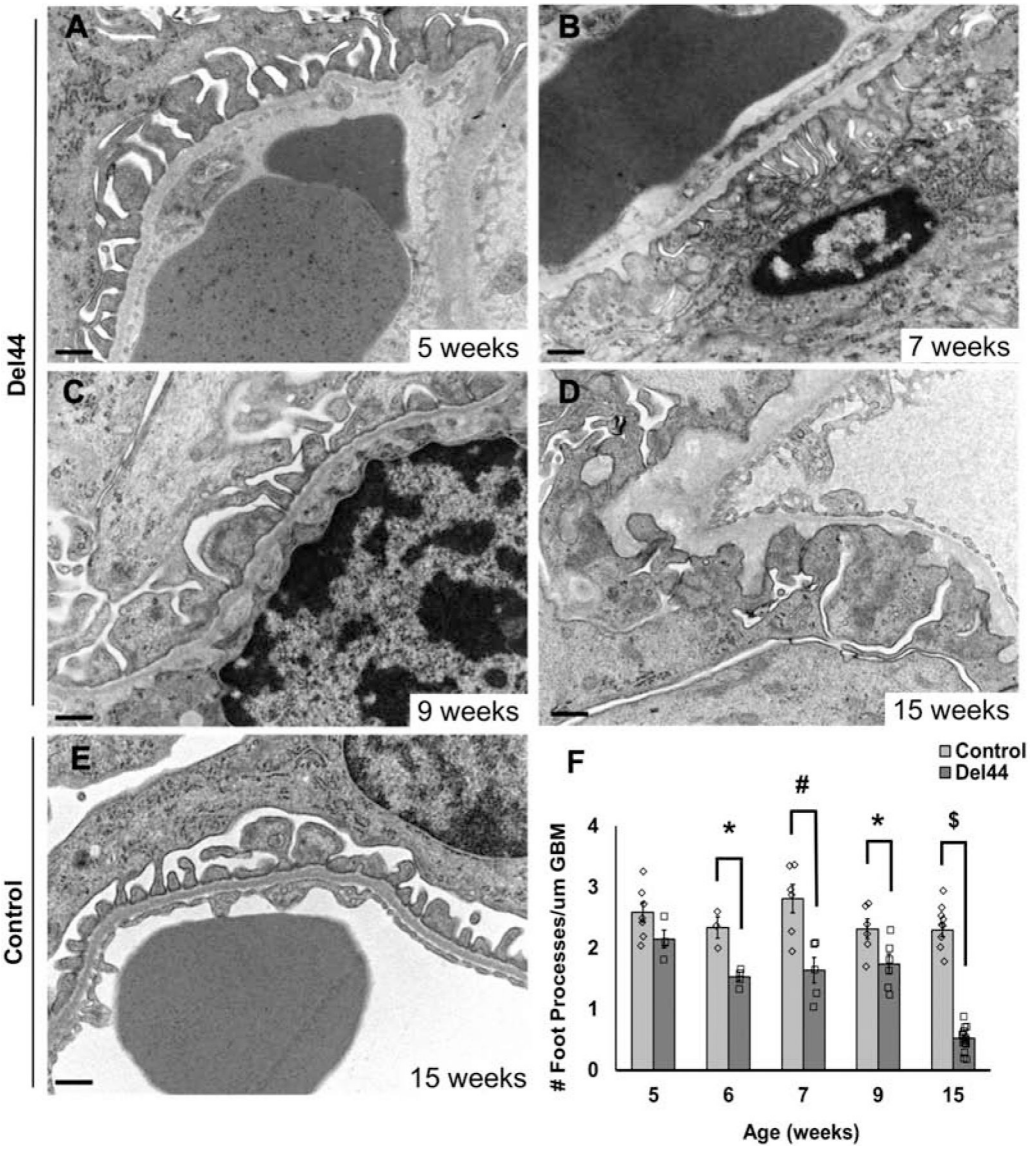

Figure 6. Transmission electron microscopy (TEM) reveals prolonged foot process maintenance in Del44 mice.

(a-c) TEM of Del44 glomerular capillary loops at 1-2 months of age (5, 7, 9 weeks) revealed widening of foot processes with maintenance of architecture and slit diaphragms, occasional GBM out-pocketing (notable in the 7-week tissue shown here), and very sparse foot process effacement concomitant with heavy and progressive albuminuria. **(d)** After 3 months of age (15 weeks) most foot processes were dramatically dysmorphic or effaced, but occasional slit diaphragms were still observable. **(e)** TEM of a glomerular capillary loop from a 15-week old control mouse. **(f)** Foot process number per μm GBM length were quantified in at least 5 micrographs taken from at least 4 different glomeruli per mouse. *, $P < 0.05$; #, $P < 0.005$; $, $P < 1 \times 10^{-9}$ by Student's *t*-test. Scale bars = 500 nm

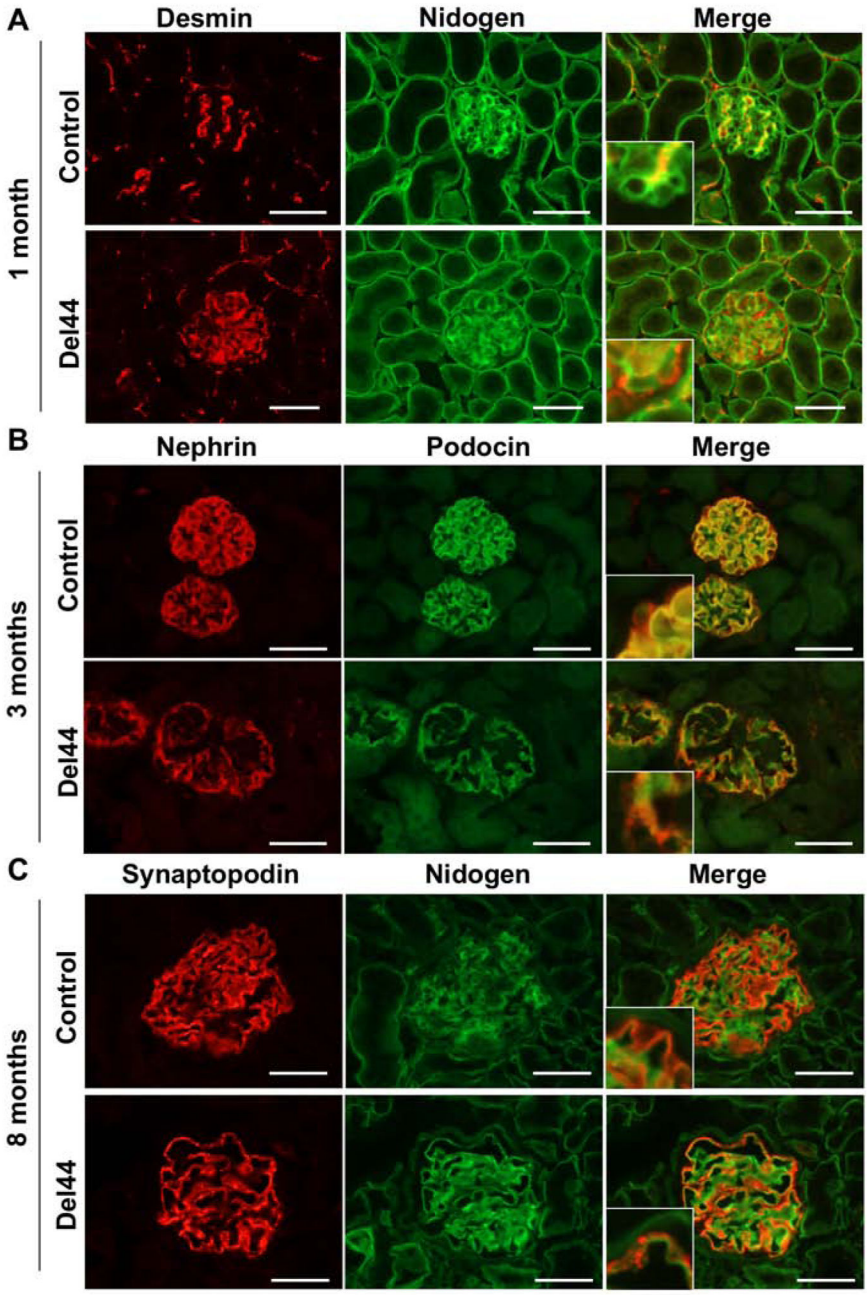

Figure 7. Immunofluorescence analysis of Del44 podocytes reveals early desmin expression but late foot process marker abnormalities.

(a) Expression of desmin, a marker of podocyte injury, in Del44 podocytes preceded proteinuria as early as 1 month of age, but expression varied among podocytes and glomeruli; n = 3-5. **(b)** Podocin and nephrin co-localized in 3 month-old Del44 glomeruli with intensities similar to controls, but with a moderately punctate appearance. Some Del44 glomerular capillary tufts appeared dilated at this age. n = 3-4 mice. **(c)** Synaptopodin expression remained robust in Del44 mice until 8 months of age, at which point the staining became punctate but exhibited intensity similar to controls; n = 3-4. Scale bars = 50 μm.

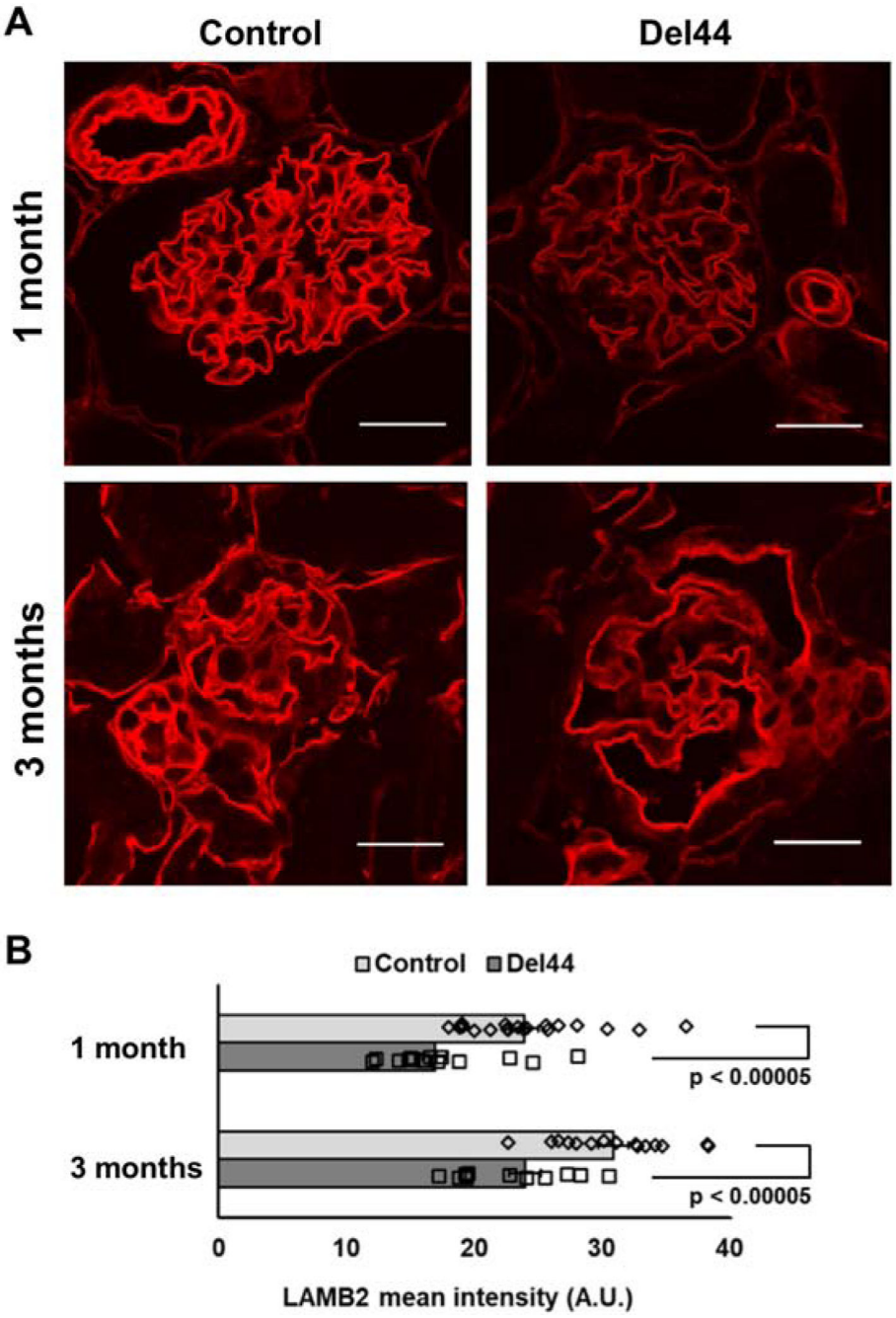

Figure 8. LAMB2-Del44 exhibits reduced expression in the GBM.

(a) Sections of kidneys aged 1 and 3 months from control and Del44 mice were stained for LAMB2 by immunofluorescence and imaged with confocal microscopy. **(b)** Anti-LAMB2 signal was ~30% reduced at 1 month and 3 months of age in Del44 glomeruli versus controls. n = 3 at each age. Statistical significance was determined with the Student's *t*-test for each age. Scale bars = 50 μm.

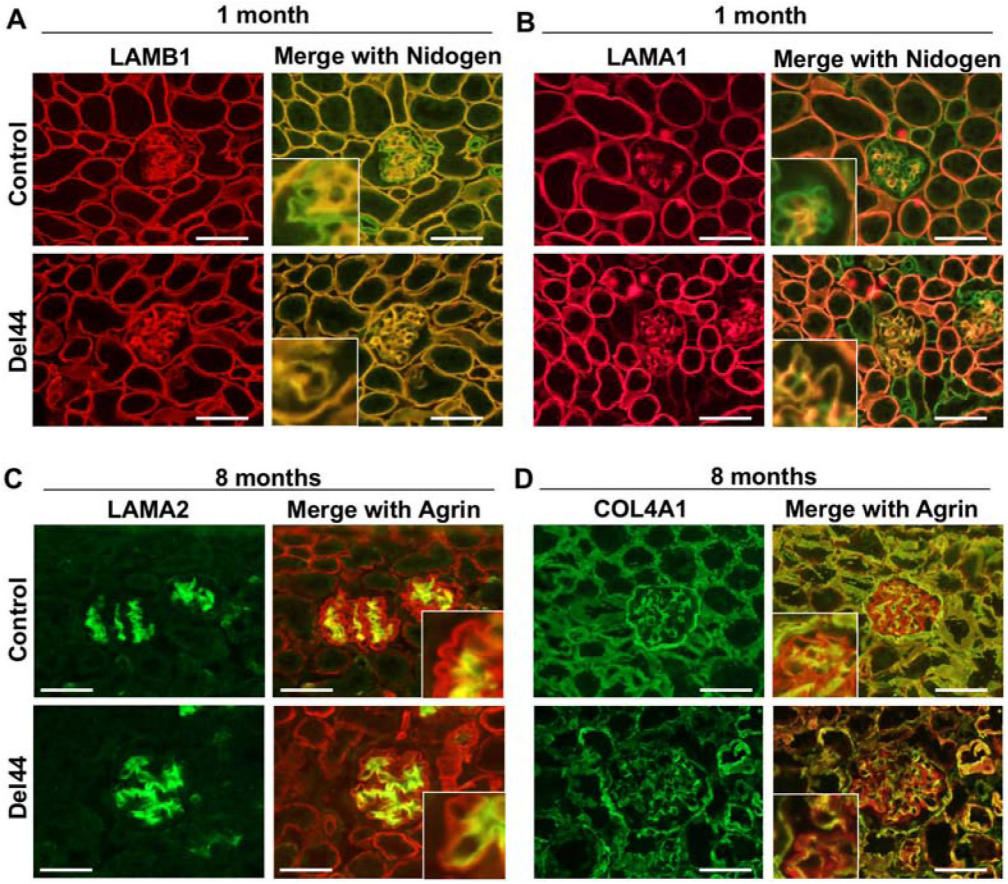

Figure 9. Aberrant expression of laminin isoforms reveals a unique molecular pathology.

(a) Del44 capillary loop GBMs exhibited accumulation of the embryonic LAMB1 isoform that co-localized with nidogen at 1 month of age preceding heavy proteinuria, suggesting a defective laminin network in Del44 mice; n = 3-4. **(b)** Accumulation of the embryonic LAMA1 isoform was also enhanced GBMs of Del44 mice at 1 month of age; n = 3-4. **(c)** LAMA2 was scarcely observed in Del44 capillary loops through 8 months of age, in contrast to *Lamb2−/−,* Alport, and *Cd151−/−* mice. n=3-4. **(d)** COL4A1 was modestly increased segmentally in the Del44 GBM at 8 months of age; n = 3-5. Scale bars = 50 μm.